Electronic Supplementary Information for

The effects of chelating N_4 ligand coordination on Co(II)-catalysed photochemical conversion of CO_2 to CO. Reaction mechanism and DFT calculations

Table of Contents

1. General experimental section

All chemicals, unless otherwise noted, were purchased from commercial sources. All solvents for synthesis, photophysical studies, and photocatalysis were of HPLC grade. The CO_2 gas (99.9%) and CH_4 gas (>99.995%) used in photocatalysis experiments were purchased from Hong Kong Oxygen & Acelylene Co., Ltd. and Hong Kong Specialty Gases Co. Ltd., respectively.

The nuclear magnetic resonance spectra were recorded on DPX-400 or DPX-300 Bruker FT-NMR spectrometer with chemical shift (in ppm) relative to tetramethylsilane (for $CDCl_3$). Mass spectra (FAB) were recorded on a Finnigan MAT 95 mass spectrometer. Mass spectra (ESI-MS) were recorded on a LCQ Classic spectrometer. Elemental analysis was performed at the Institute of Chemistry of the Chinese Academy of Sciences, Beijing.

UV/Vis absorption spectra were recorded on a Hewlett-Packard 8542A diode array spectrophotometer. Steady-state emission spectra were recorded on a SPEX 1681 Fluorolog-3 spectrophotometer. The emission lifetime measurements were performed on a Quantua Ray GCR 150-10 pulsed Nd:YAG laser system. Time-solved difference absorption spectra were recorded on LP920-KS Laser Flash Photolysis Spectrometer (Edinburgh Instruments Ltd. Livingston, UK). The excitation source was 355 nm output from a Nd:YAG laser. Solutions for photophysical studies were degassed by using a high vacuum line in a two-compartment cell with five freeze-pump-thaw cycles.

X-ray diffraction data of the single crystal were collected on a Bruker X8 Proteum diffractometer. The diffraction images were interpreted and the diffraction intensities were integrated by using the program SAINT. The crystal structure was solved by direct methods employing the SHELXS-2013 program and refined by full-matrix least-squares using the SHELXL-2013 program.[1]

Cyclic voltammetry (CV) and constant potential electrolysis were recorded on Princeton Applied Research Model 273A Potentiostat/Galvanostat. A three-electrode-system was used for the CV measurements; a glass carbon electrode and a platinum wire were applied as working electrode and counter electrode, respectively, for CV measurements; a carbon rod and a platinum net were applied as working electrode and counter electrode, respectively, for electrolysis. A non-aqueous $Ag/AgNO_3$ electrode or a saturated calomel electrode (SCE) was used as reference electrode. The ferrocene was used as internal standard when experiments using $Ag/AgNO_3$ electrode as reference electrode (formal potential for the $Ferrocene^{+/0}$ = 0.40 V *vs.*SCE).[2] The electrolyte solution is 0.1 M $[^nBu_4N]PF_6$ in CH_3CN or DMF, which was degassed by bubbling with argon or CO_2 for 20 min before measurement. The working electrode was polished with a 0.05 μm alumina paste and sonicated for 15 min before use. The conductance was measured by HI8033 conductivity meter.

2. Photocatalytic CO_2 reduction, proton reduction, and hydrogenation experiments

Photocatalytic CO_2 reduction and proton reduction: A typical procedure for photocatalysis experiment is as follows: stock solutions with certain concentration of catalyst, photosensitizer and TEA were prepared firstly. Then certain volume of the stock solutions was added into a glass tube to give a sample with total volume of 4.0 mL. The sample tube was sealed with a rubber septum and then saturated by bubbling CO_2 gas for CO_2 reduction experiments, or argon for hydrogen production experiments for 30 min in dark. The CH_4 (500 μL) was injected as the internal standard for quantitative GC-TCD analysis. Control experiment showed that no detectable CH_4 gas was formed in the course of photocatalytic CO_2 reduction under the experimental conditions. The prepared samples were set in a photo-reactor with Blue LED lamps (λ_{max} = 460 nm) as light source. The generated gas products were characterized by GC-TCD analysis (Agilent 7890A GC System) using argon as the carrier gas with a 5 Å molecular sieve column and a thermal conductivity detector. 500 μL of gas in headspace of the tube was extracted from the sample and injected into the GC. The response factor for CO/CH_4 and H_2/CH_4 were 0.30 and 3.17, respectively, under experimental conditions, which was established by calibration with known amounts of CO, H_2 and CH_4, and determined before and after a series of measurements. The TON value was calculated based on catalyst. The selectivity for CO production is calculated according to equation: selectivity (CO) = n(CO)/n(CO + H_2).

General procedure for photoinduced hydrogenation: Acetophenone (0.5 mmol, 1 equiv.), *cis*-[Co(*S*,*S*-PDP)Cl_2] (0.005 mmol, 0.01 equiv.), $Ir(ppy)_3$ (0.0015 mmol, 0.003 equiv.) were dissolved in a mixed solution of TEA (1 mL), CH_3CN (2 mL) and isopropanol (2 mL) in a 15-mL reaction tube equipped with a magnetic stirring bar. The reaction tube was sealed and the solution was bubbled by N_2 for 20 min. The as-prepared sample was set in blue LED (λ_{max} = 460 nm) photo-reactor for irradiation. After reaction for certain time, a small volume of the solution was extracted for ^{1}H NMR analysis to determine the conversion. Finally, the solvent was removed by rotary evaporation and the product was purified by column chromatography on silica gel using CH_2Cl_2 as eluent. The purified product 1-phenylethanol, obtained as a colorless liquid, was characterized by ^{1}H NMR, ^{13}C NMR, and HPLC analysis.

1-Phenylethanol: ^{1}H NMR (400 MHz, $CDCl_3$) δ 7.39–7.29 (m, 4H), 7.25 (tt, *J* = 4.3, 3.5 Hz, 1H), 4.84 (q, *J* = 6.5 Hz, 1H), 2.25 (s, 1H), 1.46 (d, *J* = 6.5 Hz, 3H). ^{13}C NMR (101 MHz, $CDCl_3$) δ 145.98, 128.63, 127.59, 125.56, 70.50, 25.28.

HPLC data of 1-phenylethanol (up, racemic; bottom, chiral)

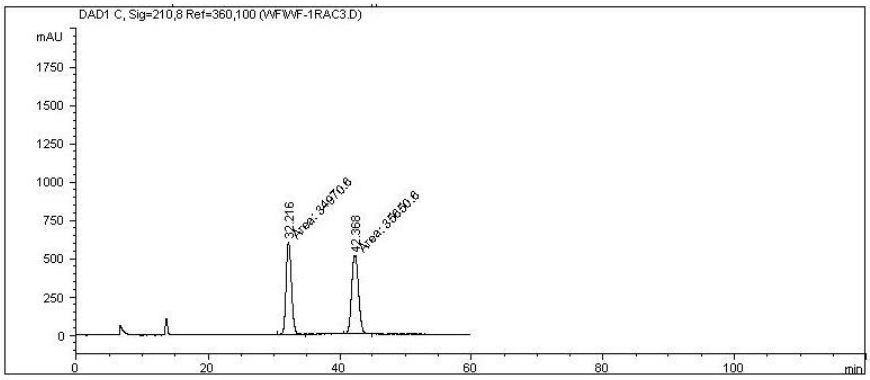


```
=====================================================================
                        Area Percent Report
=====================================================================

Sorted By             :      Signal
Multiplier            :      1.0000
Dilution              :      1.0000
Use Multiplier & Dilution Factor with ISTDs


Signal 1: DAD1 C, Sig=210,8 Ref=360,100

Peak RetTime Type  Width     Area      Height     Area
  #   [min]       [min]   [mAU*s]     [mAU]       %
----|-------|----|-------|----------|----------|--------|
   1  32.216 MM    0.9637 3.49706e4   604.80878  49.5185
   2  42.368 MM    1.1597 3.56506e4   512.34882  50.4815

Totals :                  7.06212e4  1117.15759
```

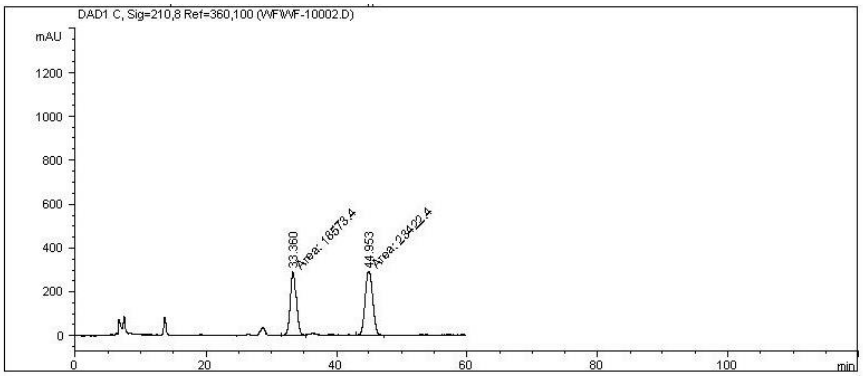


```
=====================================================================
                        Area Percent Report
=====================================================================

Sorted By             :      Signal
Multiplier            :      1.0000
Dilution              :      1.0000
Use Multiplier & Dilution Factor with ISTDs


Signal 1: DAD1 C, Sig=210,8 Ref=360,100

Peak RetTime Type  Width     Area      Height     Area
  #   [min]       [min]   [mAU*s]     [mAU]       %
----|-------|----|-------|----------|----------|--------|
   1  33.360 MM    1.0651 1.85734e4   290.62418  44.2268
   2  44.953 MM    1.3258 2.34224e4   294.44687  55.7732

Totals :                  4.19958e4   585.07104
```

3. Synthesis and characterization

The complexes $Ir(ppy)_3$,[3] and ligand **PDP, DMPDP, PDMBP, BQCN** were synthesized according to literature procedures.[4] The ligand **TDMEA** was purchased from commercial sources.

a) Ligands

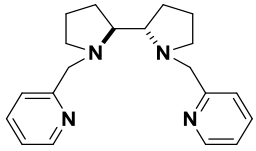

PDP: ^{1}H NMR (400 MHz, $CDCl_3$) δ 8.56–8.45 (m, 2H), 7.59 (td, *J* = 7.7, 1.7, 2H), 7.39 (d, *J* = 7.8, 2H), 7.13–7.06 (m, 2H), 4.19 (d, *J* = 14.3, 2H), 3.50 (d, *J* = 14.3, 2H), 2.99 (dt, *J* = 8.9, 4.3, 2H), 2.79 (dd, *J* = 11.2, 5.1, 2H), 2.23 (dd, *J* = 17.0, 8.6, 2H), 1.87–1.64 (m, 8H).

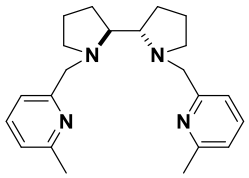

DMPDP: ^{1}H NMR (400 MHz, $CDCl_3$) δ 7.48 (t, *J* = 7.7 Hz, 2H), 7.22 (d, *J* = 7.7 Hz, 2H), 6.95 (d, *J* = 7.6 Hz, 2H), 4.15 (d, *J* = 14.6 Hz, 2H), 3.47 (d, *J* = 14.6 Hz, 2H), 3.01 (dt, *J* = 8.9, 4.3 Hz, 2H), 2.78 (d, *J* = 5.8 Hz, 2H), 2.49 (s, 6H), 2.22 (dd, *J* = 16.8, 8.4 Hz, 2H), 1.89 – 1.73 (m, 4H), 1.73 – 1.66 (m, 4H).

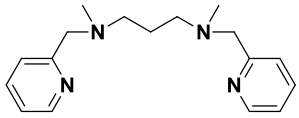

PDMBP: ^{1}H NMR (300 MHz, $CDCl_3$) δ 8.49 (d, *J* = 4.8 Hz, 2H), 7.59 (td, *J* = 7.6, 1.4 Hz, 2H), 7.34 (d, *J* = 7.8 Hz, 2H), 7.16–7.04 (m, 2H), 3.61 (s, 4H), 2.50–2.38 (m, 4H), 2.23 (s, 6H), 1.81–1.66 (m, 2H).

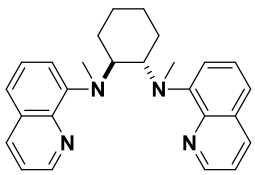

BQCN: ^{1}H NMR (400 MHz, $CDCl_3$) δ 8.81 (dd, *J* = 4.0, 1.8 Hz, 2H), 8.07 (dd, *J* = 8.3, 1.8 Hz, 2H), 7.40–7.30 (m, 4H), 7.22 (dd, *J* = 8.0, 1.0 Hz, 2H), 6.69 (d, *J* = 7.7 Hz, 2H), 4.79 (dd, *J* = 5.2, 3.4 Hz, 2H), 2.51 (s, 6H), 2.38 (d, *J* = 12.9 Hz, 2H), 1.84 (dd, *J* = 6.2, 3.0 Hz, 2H), 1.68 (d, *J* = 8.2 Hz, 2H), 1.40 (t, *J* = 9.3 Hz, 2H).

b) Complexes

The cobalt complexes **C1**-**C5** were synthesized by reaction of $CoCl_2 \cdot 6H_2O$ (1.0 equiv.) with corresponding ligands (1.0 equiv.) in CH_3OH (10 mL) at room temperature for 1 h. By removal of two-thirds of solvent, the remaining solution was set into diethyl ether vapor for recrystallization. The product was obtained as solid crystals.

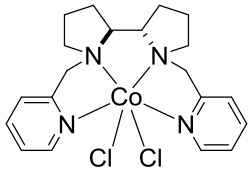

***cis*-[Co^{II}(PDP)Cl$_2$]**

C1

C1: Light purple crystals. Yield: 60%. MS (+FAB) *m/z:* 416.0 $[M - Cl]^+$. Elemental analysis Calcd. for $C_{20}H_{26}Cl_2CoN_4 \cdot 0.5H_2O$: C, 52.16, H, 5.91, N, 12.17; found: C, 52.44, H, 5.85, N, 11.92.

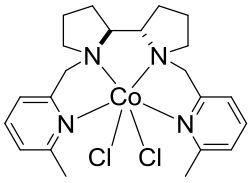

***cis*-[Co^{II}(DMPDP)Cl$_2$]**

C2

C2: Purple crystals. Yield: 50%. MS (+FAB) *m/z:* 443.8 $[M - Cl]^+$. Elemental analysis Calcd. for $C_{22}H_{30}Cl_2CoN_4 \cdot CH_3OH$: C, 53.92, H, 6.69, N, 10.93; found: C, 53.66, H, 6.63, N, 11.31.

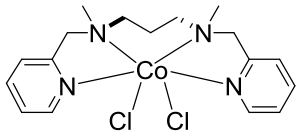

***cis*-[Co^{II}(PDMBP)Cl$_2$]**

C3

C3: Dark purple crystals. Yield: 52%. MS (+FAB) *m/z:* 378.0 [M − Cl]$^+$. Elemental analysis Calcd. for $C_{17}H_{24}Cl_2CoN_4$: C, 49.29, H, 5.84, N, 13.53; found: C, 49.28, H, 5.96, N, 13.54.

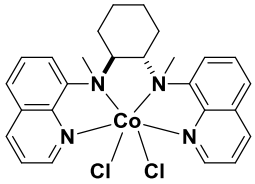

***cis*-[Co^{II}(BQCN)Cl$_2$]**

C4

C4: Light red crystals. Yield: 69%. MS (+FAB) *m/z:* 490.0 [M − Cl]$^+$. Elemental analysis Calcd. for $C_{26}H_{28}Cl_2CoN_4 \cdot 0.5CH_3CN \cdot 0.5H_2O$: C, 58.42, H, 5.54, N, 11.36; found: C, 58.08, H, 5.48, N, 11.48.

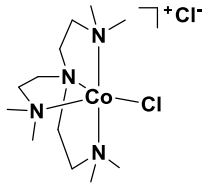

[Co^{II}(TDMEA)Cl]Cl

C5

C5: Green crystals. Yield: 70%. MS (+FAB) *m/z:* 324.0 [M − Cl]$^+$. Elemental analysis Calcd. for $C_{12}H_{30}Cl_2CoN_4$: C, 40.01, H, 8.39, N, 15.55; found: C, 39.45, H, 8.13, N, 15.32.

4. Electrochemistry

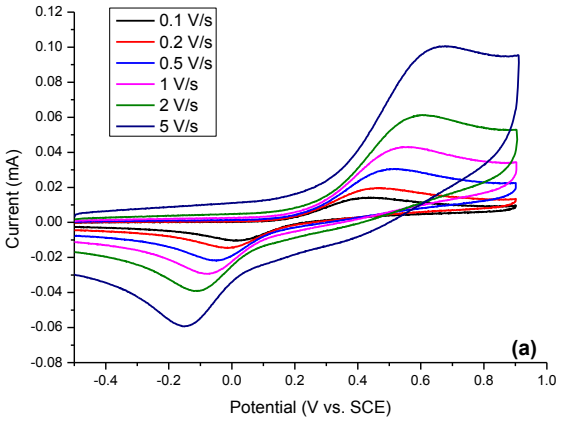

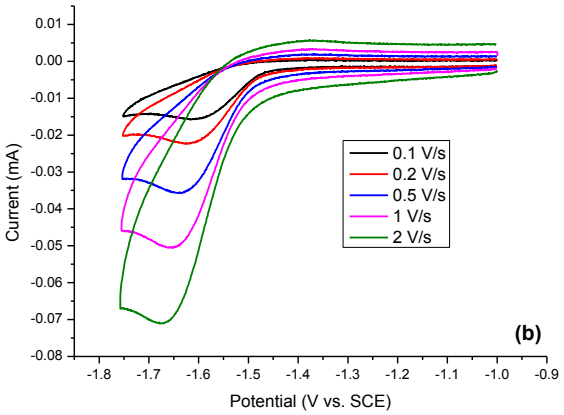

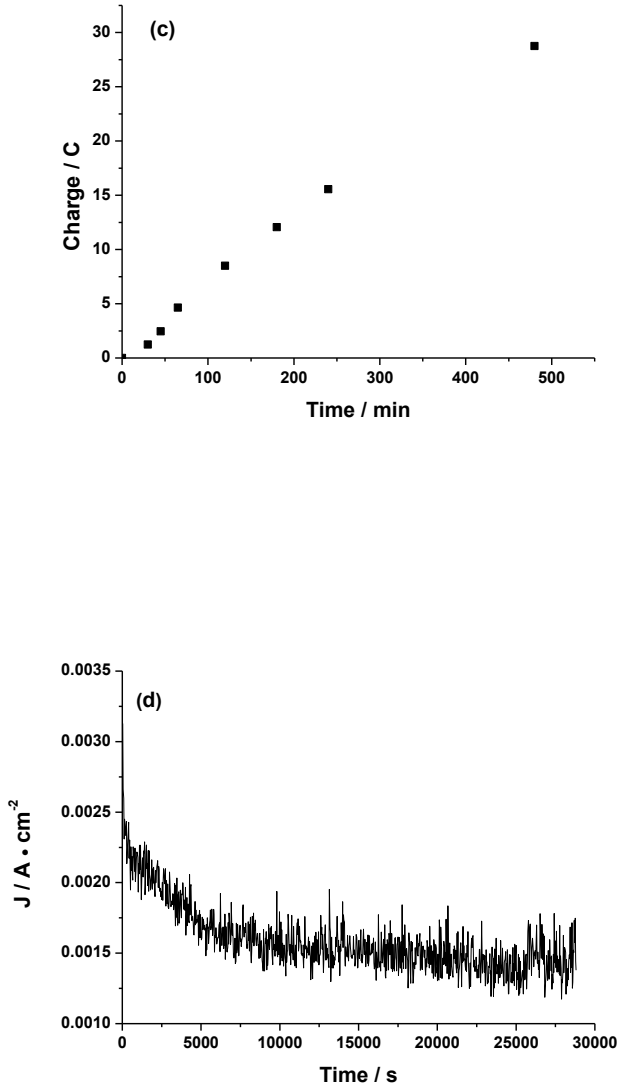

Fig. S1 cyclic voltammograms of the oxidation wave (a) and reduction wave (b) of *cis*-[Co(PDP)Cl_2] at different scan rates. Plot of charge accumulated (c) and current density (d) *vs.* time for a constant potential electrolysis in a 0.1 M [^{n}Bu_4N]PF_6 acetonitrile solution containing 1.0 mM of catalyst *cis*-[Co(PDP)Cl_2] under CO_2 atmosphere; working electrode: carbon rod.

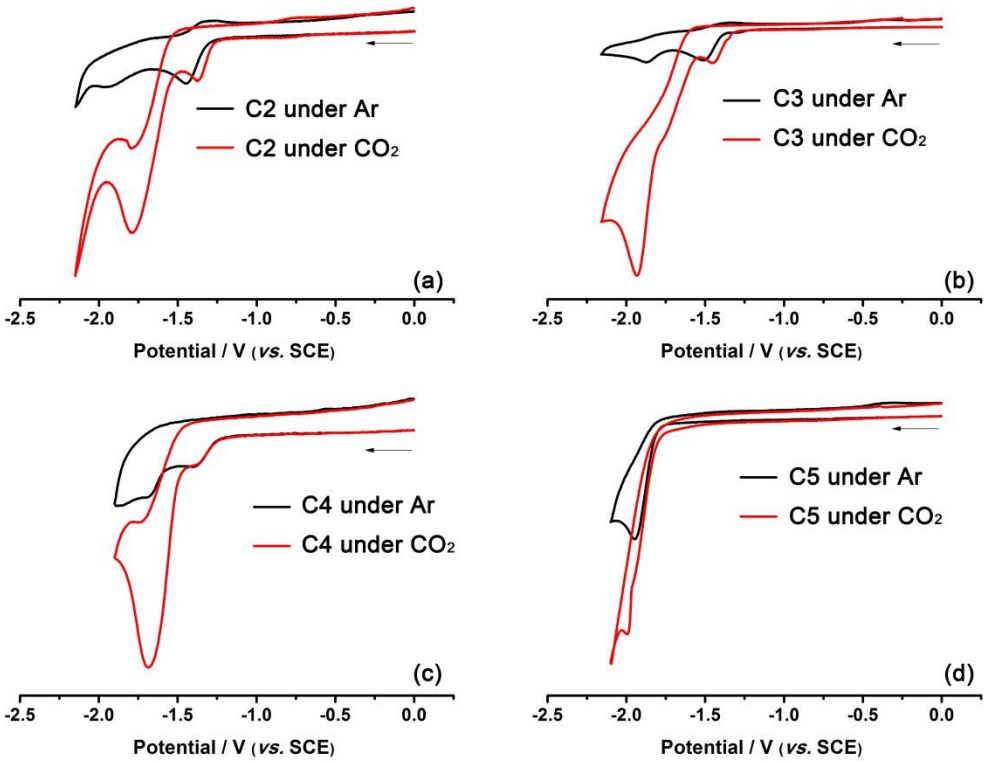

Fig. S2 Cyclic voltammograms of **C2**-**C4** in a 0.1 M [^{n}Bu$_4$N]PF$_6$ acetonitrile solution under Ar (black line) or CO_2 (red line) atmosphere

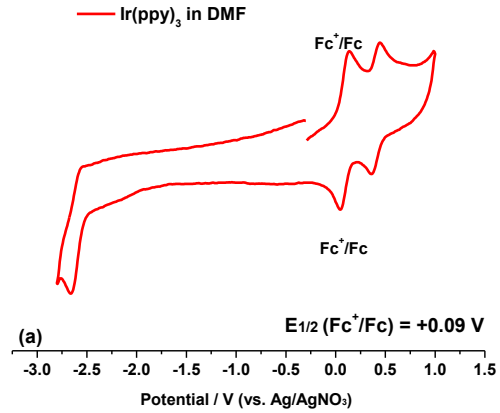

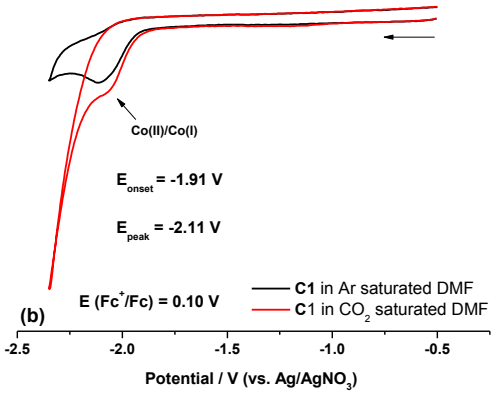

Fig. S3 (a) Cyclic voltammograms of $Ir(ppy)_3$ in a 0.1 M $[^nBu_4N]PF_6$/DMF solution under Ar; (b) cyclic voltammograms of ***cis*-[Co(PDP)Cl$_2$]** (**C**) in a 0.1 M $[^nBu_4N]PF_6$/DMF solution under Ar (black line) or CO_2 (red line) atmosphere; scan rate: 100 mV·s^{-1}.

5. UV-Vis absorption of *cis*-[Co(PDP)Cl_2]

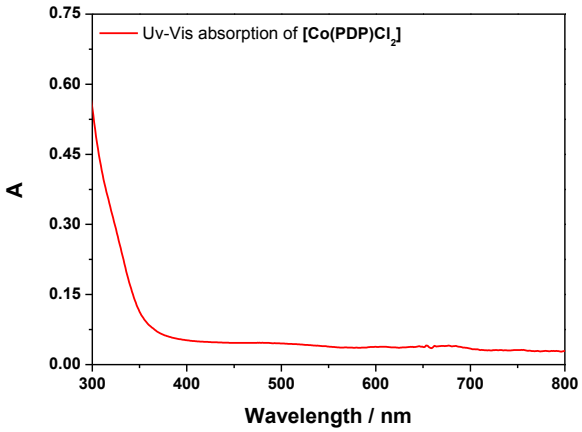

Fig. S4 UV-Vis absorption spectrum of *cis*-[Co(PDP)Cl_2] (4.00×10^{-5} M) in DMF at room temperature.

6. Quenching experiments

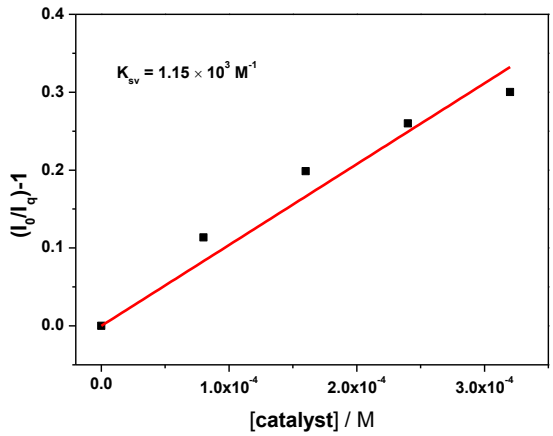

Fig. S5 Stern-Volmer equation fitting for the emission quenching of $Ir(ppy)_3$ (4.00×10^{-6} M) by *cis*-$[Co(PDP)Cl_2]$ (concentration range: 8.00×10^{-5} M - 3.20×10^{-4} M) in degassed DMF at room temperature, excited wavelength: 400 nm.

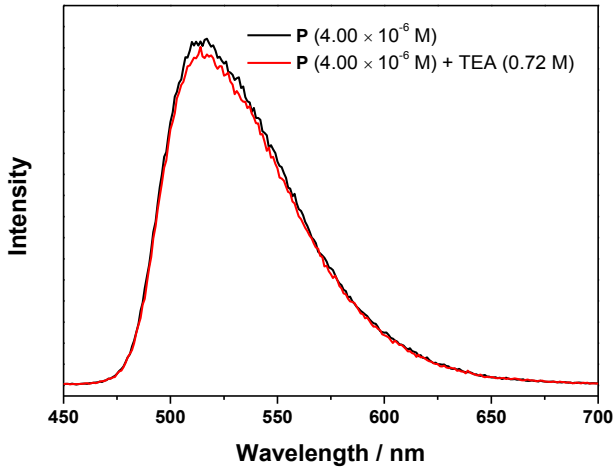

Fig. S6 Emission spectra of $Ir(ppy)_3$ (**P**) (4.00×10^{-6} M) in the absence (black line) and presence (red line) of TEA (0.72 M) in degassed DMF at room temperature, excited wavelength: 400 nm.

7. Transient absorption

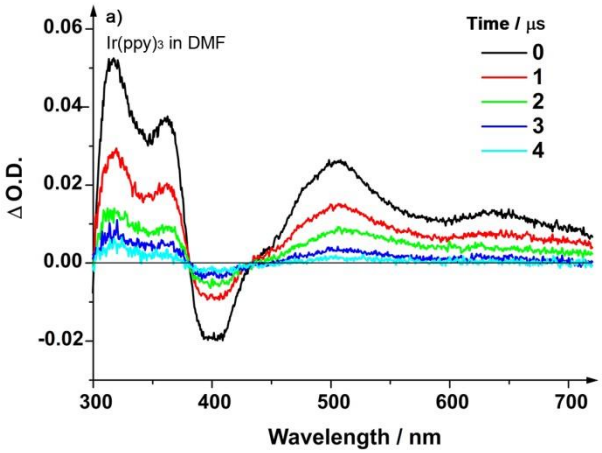

Fig. S7 Nanosecond time-resolved difference absorption spectra of $Ir(ppy)_3$ (2.00×10^{-5} M) in degassed DMF recorded from 0 to 4 µs after laser pulse excitation (355 nm).

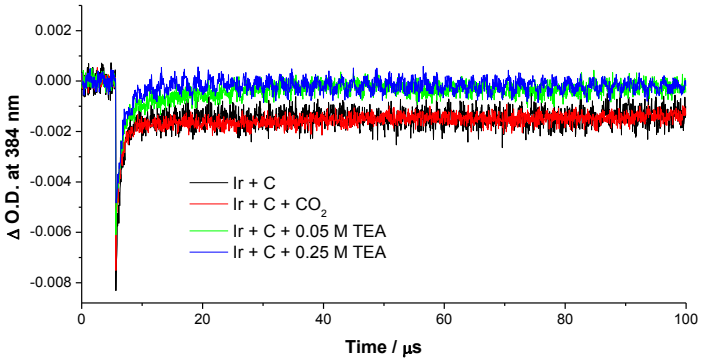

Fig. S8 Decay kinetics of the difference absorption at 384 nm after excitation (355 nm) of different solution mixtures: $Ir(ppy)_3$ (2.00×10^{-5} M) + **C** (1.00×10^{-3} M) in Ar-saturated DMF (black line); $Ir(ppy)_3$ (2.00×10^{-5} M) + **C** (1.00×10^{-3} M) in CO_2-saturated DMF (red line); $Ir(ppy)_3$ (2.00×10^{-5} M) + **C** (1.00×10^{-3} M) + TEA (0.05 M) in Ar-saturated DMF (green line); $Ir(ppy)_3$ (2.00×10^{-5} M) + **C** (1.00×10^{-3} M) + TEA (0.25 M) in Ar-saturated DMF (blue line); (**P** = $Ir(ppy)_3$, **C** = *cis*-[$Co(PDP)Cl_2$]).

8. DFT calculations

Molecular structures were optimized by the M06L functional.[5] Frequency calculations at the same level were carried out to corroborate all of the stationary points as minima (no imaginary frequency) and to compute free energies at 298.15 K. The 6-31G* Pople basis set[6] was employed for all the atoms except for Co atom with effective core potential (ECP) type basis set LANL2DZ.[7] The solvent effect was included by the single point calculations for all the optimized gas-phase structures with self-consistent reactions field (SCRF) based on the polarizable continuum model (PCM)[8] in which DMF was the solvent as the experimental condition. The functional of M06[9] was applied in the single point calculations to compute energy; 6-311+G* basis set[10] was applied on all the atoms except for Co atom with the Hay-Wadt relativistic effective core potentials (RECPs) LANL2TZ(f).[11] In our simulation, the free energy of proton was taken as -11.75 eV in DMF,[12] in which its solvation free energy was taken from computation with M062X/6-311++G(d,p).[13] The solvation free energy for Cl^- in DMF was taken from experimental values.[14] All the simulations were performed by Gaussian 09 packages.[15]

9. Crystal structures

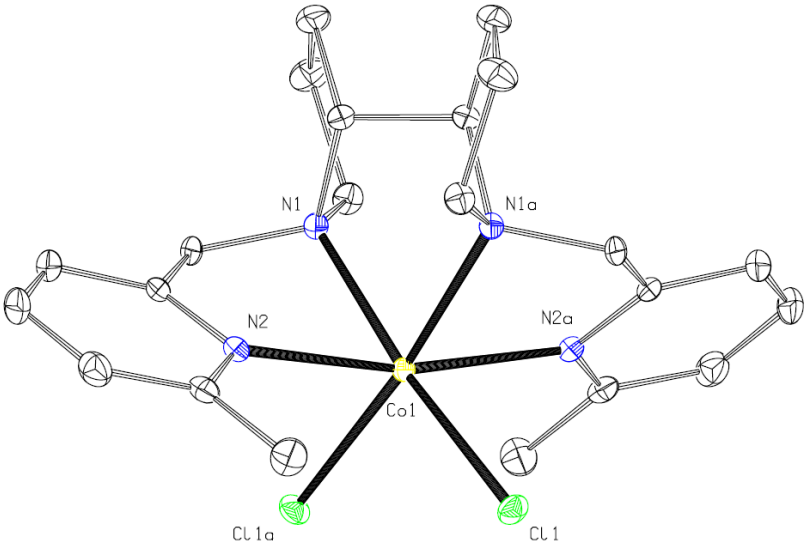

C2

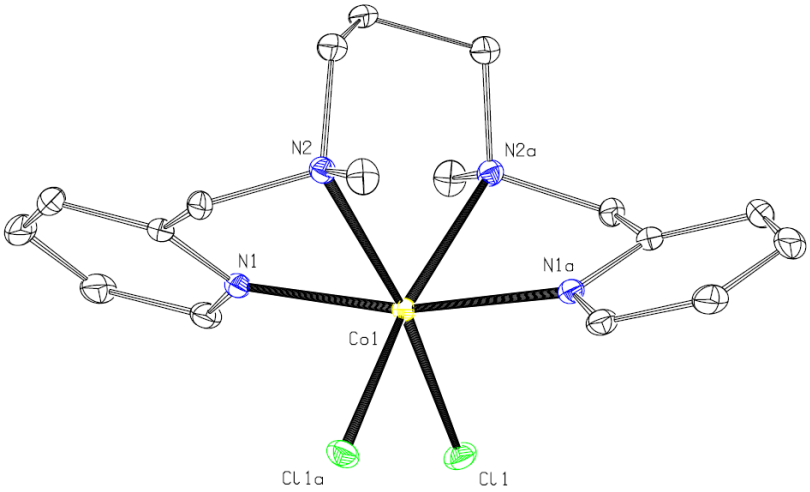

C3

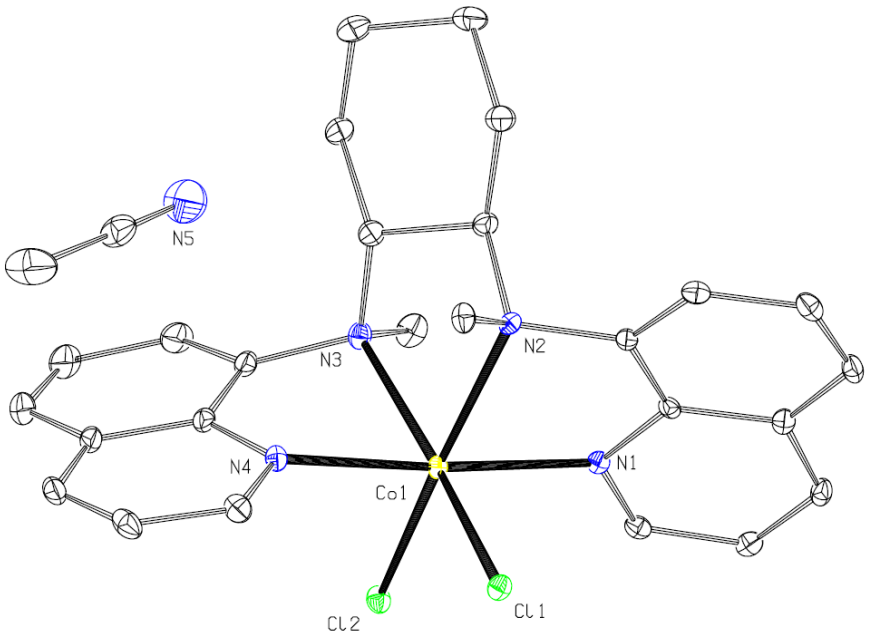

C4

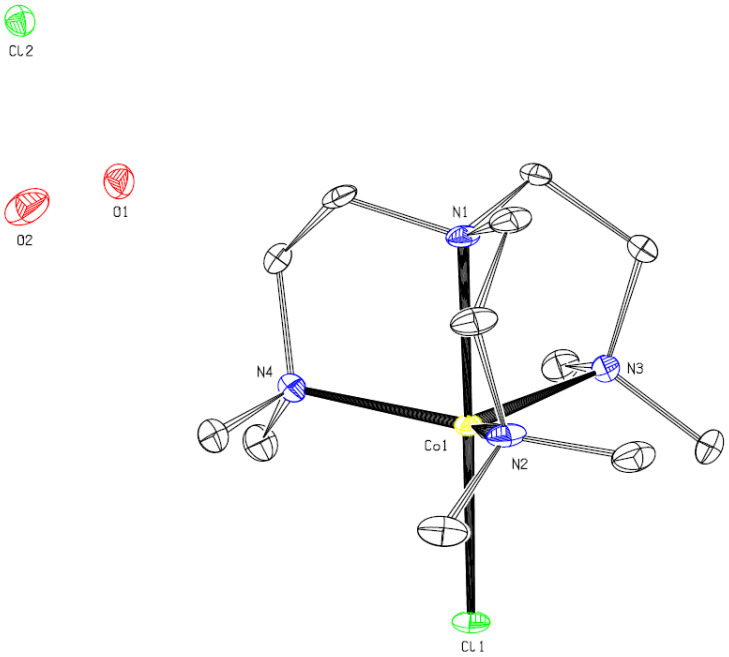

C5

10. References

1. G. M. Sheldrick, *Acta Crystallogr. Sect. A*, 2008, **64**, 112-122.

2. N. G. Connelly, W. E. Geiger, *Chem. Rev.*, 1996, **96**, 877-910.

3. K. Dedeian, P. I. Djurovich, F. O. Garces, G. Carlson, and R. J. Watts, *Inorg. Chem.*, 1991, **30**, 1685-1687.

4. (*a*) M. S. Chen and M. C. White, *Sciences*, 2007, **318**, 783-787; (*b*) J. England, G. J. P. Britovsek, N. Rabadia and A. J. P. White, *Inorg. Chem.*, 2007, **46**, 3752-3767; (*c*) D. S. Kissel, J. Florián, C. C. McLauchlan and A. W. Herlinger, *Inorg. Chem.*, 2014, **53**, 3404-3416.

5. Y. Zhao and D. G. Truhlar, *J. Chem. Phys.*, 2006, **125**, 194101.

6. (*a*) P. C. Hariharan and J. A. Pople, *Theor. Chim. Acta*, 1973, **28**, 213-222; (*b*) M. M. Francl, W. J. Pietro, W. J. Hehre, J. S. Binkley, M. S. Gordon, D. J. DeFrees and J. A. Pople, *J. Chem. Phys.*, 1982, **77**, 3654-3665.

7. P. J. Hay and W. R. Wadt, *J. Chem. Phys.*, 1985, **82**, 299-310.

8. (*a*) S. Miertuš, E. Scrocco and J. Tomasi, *Chem. Phys.*, 1981, **55**, 117-129; (*b*) J. Tomasi, B. Mennucci and R. Cammi, *Chem. Rev.*, 2005, **105**, 2999-3094.

9. Y. Zhao, D. Truhlar, *Theor. Chem. Acc.*, 2008, **120**, 215-241.

10. (*a*) R. Krishnan, J. S. Binkley, R. Seeger and J. A. Pople, *J. Chem. Phys.*, 1980, **72**, 650-654; (*b*) T. Clark, J. Chandrasekhar, G. W. Spitznagel and P. V. R. Schleyer, *J. Comput. Chem.*, 1983, **4**, 294-301.

11. L. E. Roy, P. J. Hay, R. L. Martin, *J. Chem. Theory Comput.*, 2008, **4**, 1029-1031.

12. (*a*) C. P. Kelly, C. J. Cramer and D. G. Truhlar, *J. Phys. Chem. B*, 2006, **111**, 408-422; (*b*) B. T. Psciuk, R. L. Lord, B. H. Munk and H. B. Schlegel, *J. Chem. Theory Comput.*, 2012, **8**, 5107-5123.

13. H. Farrokhpour and M. Manassir, *J. Chem. Eng. Data*, 2014, **59**, 3555-3564.

14. E. A. Gomaa, *Global Adv. Res. J. Chem. Mater. Sci.*, 2012, **1**, 035-038.

15. R. D. Gaussian 09, M. J. Frisch, G. W. Trucks, H. B. Schlegel, G. E. Scuseria, M. A. Robb, J. R. Cheeseman, G. Scalmani, V. Barone, B. Mennucci, G. A.

Petersson, H. Nakatsuji, M. Caricato, X. Li, H. P. Hratchian, A. F. Izmaylov, J. Bloino, G. Zheng, J. L. Sonnenberg, M. Hada, M. Ehara, K. Toyota, R. Fukuda, J. Hasegawa, M. Ishida, T. Nakajima, Y. Honda, O. Kitao, H. Nakai, T. Vreven, J. A. Montgomery, Jr., J. E. Peralta, F. Ogliaro, M. Bearpark, J. J. Heyd, E. Brothers, K. N. Kudin, V. N. Staroverov, R. Kobayashi, J. Normand, K. Raghavachari, A. Rendell, J. C. Burant, S. S. Iyengar, J. Tomasi, M. Cossi, N. Rega, J. M. Millam, M. Klene, J. E. Knox, J. B. Cross, V. Bakken, C. Adamo, J. Jaramillo, R. Gomperts, R. E. Stratmann, O. Yazyev, A. J. Austin, R. Cammi, C. Pomelli, J. W. Ochterski, R. L. Martin, K. Morokuma, V. G. Zakrzewski, G. A. Voth, P. Salvador, J. J. Dannenberg, S. Dapprich, A. D. Daniels, Ö. Farkas, J. B. Foresman, J. V. Ortiz, J. Cioslowski and D. J. Fox, *Gaussian, Inc.*, Wallingford CT, 2009.